Assessment and validation of wave excitation force estimators in operative conditions

Control Engineering Practice 151 (2024) 106019

Contents lists available at ScienceDirect

Control Engineering Practice

journal homepage: www.elsevier.com/locate/conengprac

Assessment and validation of wave excitation force estimators in operative conditions

Guglielmo Papini [a,*], Edoardo Pasta [a], Yerai Peña-Sanchez [b], Facundo D. Mosquera [c], Demián García-Violini [e,f], Francesco Ferri [d], Nicolás Faedo [a]

[a] Marine Offshore Renewable Energy Lab, Department of Mechanical and Aerospace Engineering, Politecnico di Torino, Turin, Italy
[b] Fluid Mechanics Department, Mondragon University, Mondragon, Spain
[c] Instituto de Investigaciones en Electrónica, Control y Procesamiento de Señales, Universidad Nacional de La Plata, Buenos Aires, Argentina
[d] Department of the Built Environment, Aalborg University, Aalborg, Denmark
[e] Departamento de Ciencia y Tecnología, Universidad Nacional de Quilmes, Bernal, Argentina
[f] CONICET, Buenos Aires, Argentina

ARTICLE INFO

Keywords:
Wave energy
Experimental validation
System identification
Excitation force estimators

ABSTRACT

For a reliable development of energy-maximising optimal control strategies in wave energy, wave excitation force estimators are fundamental components in the control loop, since the optimality of the solution depends on their precision. In the control deployment phase, it is necessary to test the precision of wave estimates to assess the eventual margin of improvement for optimal energy extraction. Nonetheless, current strategies for wave estimator validation are based on the possibility of repeating with high precision the wave signal, and blocking the device in a predefined position, assumptions which are possible only in certain test facilities. This study proposes a novel estimator validation strategy, termed *closed-loop validation*, based on the analysis of the system motion only, which is suitable for testing excitation force estimators under realistic (open-sea) conditions. For this purpose, two excitation force observers, based on a random walk and a harmonic oscillator wave description, are developed, on the basis of the energy conversion device identified model. In particular, the device is a WaveStar prototype at the Aalborg University facility tank, in Denmark. The observers (and the identified model) are validated under irregular sea states, with both the classical and the proposed scheme, proving the effectiveness of the latter in demonstrating the excitation force estimator performance without requiring a direct force measurement.

1. Introduction

The actual context of climate change, caused by the increasing emission level of carbon dioxide, has driven global policy-makers to search for alternative, fossil-free energy sources. In this scenario, renewable power systems, such as wind, solar, and wave energy, have gained significant attention both from the industrial and academic worlds (Twidell, 2021), driven by the structural independence of such systems from carbon-based fuels, and from the theoretically inexhaustible nature of the primary energy sources, *i.e.* the natural resource of wind, solar radiation and wave motion. Nonetheless, the global implementation of such technologies is still facing structural limitations, such as the non-constant energy source availability, or the geographical restrictions in which the source itself is available.

In this context, wave energy shows significant potential due to the huge energetic content of the wave motion, and the global spread of the power source, *i.e.* the sea (Mork, Barstow, Kabuth, & Pontes, 2010). The devices in charge of converting the wave motion into electrical energy are termed wave energy converters (WECs), and commonly comprise a floating buoy, and an electro-mechanical motor/generator system referred to as power take-off (PTO), which converts the kinetic energy associated with the buoy motion into electrical power. Notwithstanding, wave energy is still facing economic viability challenges, which are hindering the commercialisation of WECs. A key stepping stone, in this path, is the development of energy-maximising optimal control (OC) strategies (Ringwood, Zhan, & Faedo, 2023), whose objective is that of maximising the energy extracted from the device under the current sea state conditions, while maintaining physical constraints on the device motion and the PTO actuation limits. Some examples of popular OC algorithms in wave energy are model predictive control (MPC) (Papini, Paduano et al., 2023) or moment-based control (Faedo, Giorgi, Ringwood, & Mattiazzo, 2022), which

* Corresponding author.
E-mail address: guglielmo.papini@polito.it (G. Papini).

https://doi.org/10.1016/j.conengprac.2024.106019
Received 4 December 2023; Received in revised form 7 May 2024; Accepted 12 July 2024
Available online 25 July 2024

structurally feature energy-maximising and constraint handling abilities. With particular reference to the system described in detail in Section 2, and keeping in mind that results can be easily extended to a more generic WEC family, the optimal control problem (OCP) can be written as

$$\begin{aligned} &\min_{u} J, \quad J = \int_{T_p} u(t)\dot{z}(t)\mathrm{d}t \\ &\quad s.t. \\ &\quad \text{WEC dynamics,} \\ &\quad \text{Physical constraints,} \end{aligned} \tag{1}$$

where the cost function J is the energy extracted over the time horizon $T_p \subseteq \mathbb{R}^+$, $\dot{z}(t) \in \mathbb{R}$ is the velocity associated with the WEC motion, and $u(t) \in \mathbb{R}$ is the control torque implemented by the PTO. Due to the computational burden associated with solving problem (1) in real-time, which is also connected with the well-known issues of wave forecast and estimation (Faedo, Peña-Sanchez, & Ringwood, 2020; Li, Weiss, Mueller, Townley, & Belmont, 2012), the most common approach is to solve (1) in a receding-horizon fashion, *i.e.* at each control sampling instant solving the OCP over the future time horizon T_p and applying the first set of optimal control actions to the system, according with the specific policy.

As discussed in Faedo et al. (2022), Scruggs, Lattanzio, Taflanidis, and Cassidy (2013), the solution of (1) depends on the future values assumed by the wave excitation signal comprised in the WEC dynamics over the prediction time window T_p, which in practice are not available. A common solution is to forecast the behaviour of the wave, on the basis of past and current force estimates, by exploiting regressor systems (Papini, Peña-Sanchez, Pasta, & Faedo, 2023), and use the computed wave forecast in the optimisation problem formulation, thus approximating the exact solution of (1). Nonetheless, these methods require a precise knowledge of the instantaneous wave excitation force/torque, which in practice cannot be achieved via physical measurements, and has to be retrieved using wave estimation techniques (Peña-Sanchez, Windt, Davidson, & Ringwood, 2019). As such, the estimate quality considerably influences the performance (extracted energy, in particular) of the OC strategy, hence constituting a fundamental and critical stage in the development of effective energy-maximising, optimal controllers. Given such considerations, the principal feature of a wave excitation force observer resides in the precision of force estimation. This performance parameter is relatively trivial to assess in a numerical simulation environment, by comparing the system input force defined at the simulation setup stage, and the obtained force estimate. Nonetheless, when it comes to experimental tests, additional issues can arise. One main problem is the actual system excitation signal unavailability since, even in controlled environments (*i.e.* wave tank facilities), there are no instruments for directly measuring the instantaneous force acting on the WEC hull, unless additional considerations are put in place. As discussed in detail in Section 5.3, a common procedure to overcome such limitation consists of blocking the WEC system in equilibrium position during wave experimental simulation, and measuring the excitation force with a mechanical sensor (*e.g.* a torque meter/load cell attached to the PTO). Once the measurement is available, the estimator is tested under the measured wave profile with the idea of reproducing the system velocity trajectory as if any blocking mechanism had been applied in the previous test. If the estimation error between the measured torque/force and the estimated signal is low, the estimator performance is validated. Nonetheless, the described procedure is based on the assumptions of blocking the device and reproducing perfectly a predetermined wave elevation profile, which in practice is not available for full-scale devices operating in the open sea.

Given this crucial aspect, this study proposes a novel wave excitation force estimator validation strategy capable of overcoming the state-of-the-art validation techniques' structural limitations. In particular, the proposed structure is based on the *WEC instantaneous motion analysis*, thus eliminating both the device locking requirement, and the associated condition on wave signal repeatability. The efficiency of the proposed validation strategy is tested experimentally as part of the campaign described in Faedo, Peña-Sanchez, Pasta, et al. (2023), on two wave excitation force observers (whose design is treated in detail between Sections 3 and 4), and consequently compared with the standard method for assessing its theoretical and experimental consistency. This study is structured as follows. Section 2 describes the experimental setup of the device, the wave tank, and the connected instruments. Section 3 treats the experimental mathematical model employed for the excitation force observers designs. Section 4 describes the mathematical details of the excitation force estimators implementation. In Section 5, the observers performance are tested, and a comparison is offered between standard and proposed validation procedures. Finally, Section 6 discusses the experimental results and points out the observed features of the novel validation technique.

1.1. Notation

Within this work the symbols $\mathbb{N}$, $\mathbb{R}$ and $\mathbb{C}$ are used for the set of natural, real and complex numbers, respectively. The apex notation $\{\cdot\}^\mathsf{T}$ stands for the matrix transpose operation, while $\{\hat{\cdot}\}$ denotes a signal estimate. The symbols $\dot{z}$, v_θ and $\dot{\theta}$ are used equivalently, and stand for the angular velocity of the arm around hinge A (see Fig. 1). The symbol 0 is used to indicate the zero element, where the dimensions (*i.e.* corresponding space) is always clear from the context, while $\mathbf{1}_a \in \mathbb{R}^a, a \in \mathbb{N}$, is employed for indicating a row vector of dimension a with all entries equal to 1. The symbol $\mathbb{I}_a \in \mathbb{R}^a$ indicates the $a-$dimensional identity matrix. Given a generic function f, its Laplace transform (provided its existence) is denoted with $F(s), s \in \mathbb{C}$, while its Fourier transform is indicated with the argument restriction to the set of complex numbers with zero real part, namely $F(j\omega), \omega \in \mathbb{R}$.

2. Experimental tank and instrumentation setup

This section describes the experimental facility setup, which is physically placed within Aalborg University, Denmark. The device, which is depicted in Fig. 1, is a 1:20 scale prototype of the WaveStar WEC device (Kramer, Marquis, & Frigaard, 2011) unit, specifically designed by Aalborg University, is tested within a broader experimental campaign described in Faedo, Peña-Sanchez, Pasta, et al. (2023). The considered system comprises a hemispherical composite floater, which is supported with a steel arm, free to move about the lower vertical support hinge, with an equilibrium position with respect to the horizontal axis of approximately $30°$. The PTO system, which is linked to the rotating arm and the upper structure rotational hinge, is an electrical, direct drive linear actuator (*LinMot Series P01-37 x 240F*). The PTO is controlled with a *LinMot E1200* driver, which features a force rating of ± 200 [N]. The remaining parameters characterising the device are presented in Table 1.

Concerning the measurement system, the translation connected with the linear motor is measured by means of a laser sensor (*MicroEpsilon ILD-1402-600*). The motor applied force is measured with a specific load cell (*S-beam Futek LSB302*) mounted in between the actuator end and the arm upper link. The floater is equipped with a dual-axis accelerometer (*Analog Devices ADXL203EB*), used with the precise scope of obtaining the floater angular motion (position and velocity) about the lower arm joint. In particular, the angular dynamics are retrieved with a combination of the laser sensor and the accelerometer measures, via standard sensor fusion. For data acquisition and control deployment, a Speedgoat®real-time device, which is connected via Ethernet cable with a Matlab Simulink®environment is used, deployed on a dedicated target PC. The acquisition system works consistently at a sampling frequency of 200 [Hz] (see Table 2).

The tank facilities comprise a basin of 19.3 [m] length, 14.6 [m] width, and 1.5 [m] depth, while the active testing area is a rectangle

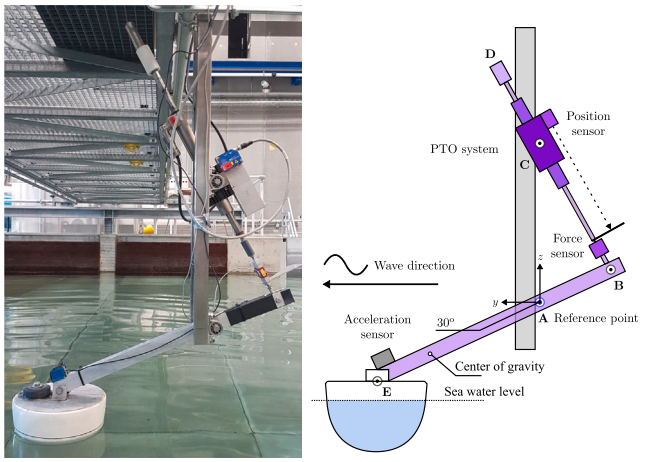

Fig. 1. Schematic of the 1:20 scale version of the WaveStar WEC, employed in the experimental campaign. Image adapted from Faedo et al. (2023).

Table 1
WaveStar 1:20 scale physical parameters, adapted from Faedo, Peña-Sanchez, Garcia-Violini et al. (2023).

Parameter	Assumed value
Measure between A and C	0.200 [m]
Measure between A and B	0.412 [m]
Measure between B and C	0.381 [m]
Measure between A and E	0.484 [m]
Arm square section side length	4.2 [cm]
Hemispherical floater diameter[1]	0.256 [m]
Arm mass	1.157 [Kg]
Arm inertia moment	0.060 [Kg m^2]
Draft	0.110 [m]
Floater inertia moment	1 [Kg m^2]
Floater mass	4 [Kg]

[1] Value referred at sea water level, in equilibrium position.

Table 2
Measurement uncertainties connected with the instrumentation setup. Table adapted from Faedo, Peña-Sanchez, Pasta, et al. (2023).

Physical component	Device name	Measure	Uncertainty
Linear motor	LinMot Series P01-37 × 240F	PTO linear position	±0.05 [mm]
Laser sensor	MicroEpsilon ILD-1402-600	PTO linear position	±80 [μm]
Load cell	S-beam Futek LSB302	Force applied in B	±0.125 [N]
Accelerometer	Analog Devices ADXL203	Floater acceleration in E	±0.01 [m/s^2]
Wave gauges	VTI WG-8CH	Wave elevation	±0.04 [mm]

of 13 [m] length and 8 [m] width. The sea conditions employed for testing the proposed strategies are generated with an advanced wavemaker. Such a device is made of 30 pads (designed by *VTI systems*) distributed along the tank width, each one controlled separately, and features active absorption and high-accuracy repeatability abilities. In this study, the tank water depth is fixed to 0.9 [m], and the wavemaker is set to generate waves in a parallel direction with the WEC lower arm, *i.e.* long-crested waves.

3. Experimental mathematical modelling

Within this section, the theoretical framework behind the system identification procedure adopted is discussed, which provides a *representative* linear representation of the prototype system, leveraging the available experimental measurements. Though the WEC system is inherently a nonlinear system, the state-of-the-art wave excitation force estimation architectures are based on a linear model representation of the WEC system for design and synthesis. Consequently, the proposed identification procedure is designed to account, with some degree of uncertainty, any bias introduced by nonlinear effects by means of the 'averaging' step in (4) while, at the same time, to provide a numerically tractable (yet representative) linear structure for the studied WEC system.

Within linear potential flow theory (Falnes & Kurniawan, 2020), the input–output torque-to-angular velocity response can be characterised with linear mapping $G : \mathbb{C} \to \mathbb{C}, s \mapsto G(s)$, for describing the WEC rotational dynamics around hinge A in Fig. 1

$$V_\theta(s) = G(s)\left[D(s) - U(s)\right], \tag{2}$$

where $\theta(t) \in \mathbb{R}$ is the angular displacement, $d(t) \in \mathbb{R}$ is the wave excitation torque exerted by the wave motion, and $u(t) \in \mathbb{R}$ is the control torque implemented by the PTO, adequately reported on the hinge A reference system.

Remark 1. The term $d(t)$ in (2) is an exogenous input, *i.e.* excites the system as an external, uncontrollable, disturbance. Additionally, from a spectral point of view, such a signal is similar to the control action $u(t)$, consequently making the separation task of the two quantities not trivial.

For characterising the map in (2), a black box system identification approach is pursued, *i.e.* the dynamical model is obtained on the basis of input/output (I/O) data, without additional assumptions on the model structure.

Remark 2. Standard WEC modelling approaches among the literature rely on a parametric system description, whose parameters are directly dependent on the physical properties of the system, and the hydrodynamic response is virtually always computed by the so-called boundary element method-based software (Babarit & Delhommeau, 2015). Notwithstanding, such procedure introduces two significant uncertainty sources in this scenario: the hydrodynamic model precision (*e.g.* the omission of non-ideal effects, parametric uncertainty in the hydrodynamic response, among others) and any unmodelled subsystem dynamics, such as the potential effect of the PTO linear motor, which ultimately influence the overall system response.

Driven by the reasoning presented in Remark 2, a system identification procedure is proposed for obtaining a control-oriented linear model of the WEC prototype, which can accurately describe the system's dynamics in the considered sea states.

In this section, the procedure employed for obtaining experimentally the mapping $G(s)$ in (2) is presented.

Let the signal $d^\star(t) \in \mathbb{R}$ be a normalised down-chirp (which choice, with respect to the up-chirp case, is connected with the minimisation of the reflected waves in the basin during the identification tests, see Faedo, Peña-Sanchez, Garcia-Violini et al. (2023)) of time length T_{dc}, properly designed to excite the system in the frequency range $\Delta \subset \mathbb{R}$. Define $\Gamma = \{\Gamma_i\}_{i=1}^{N_\Gamma}$ as the set of identification signal amplitudes, where $N_\Gamma \in \mathbb{N}$ is the associated cardinality. Leveraging this definition, the set of input signals employed for system identification is denoted as $\mathcal{D} = \{\Gamma_i d^\star(t)\}_{i=1}^{N_\Gamma}$. The overall procedure applies, in still water basin conditions (*i.e.* when the wavemaker is inactive and there are no waves inside the tank), the identification signals by means of the PTO system, and subsequently records the corresponding outputs (angular velocities v_θ), which set is denoted as $\mathcal{V}_\theta = \{v_{\theta i}(t)\}_{i=1}^{N_\Gamma}$.

Let the empirical transfer function estimate (ETFE) relative to each I/O pair $\left(\Gamma_i d^\star(t), v_{\theta i}(t)\right) \in \mathcal{D} \times \mathcal{V}_\theta$, namely $\hat{G}_i : \mathbb{C} \to \mathbb{C}$, $j\omega \mapsto \tilde{G}_i(j\omega)$, be defined as

$$\tilde{G}_i(j\omega) = V_{\theta i}(j\omega)/\Gamma_i D^\star(j\omega), \quad i \in N_\Gamma. \tag{3}$$

Given the ETFE structure in (3), it is possible to obtain a model which is representative, in an average fashion, of the system dynamics under the test design conditions. Such a mapping, namely $\bar{G}(j\omega) : \mathbb{C} \to \mathbb{C}, j\omega \mapsto \bar{G}(j\omega)$ can be computed as

$$\bar{G}(j\omega) = \frac{1}{N_\Gamma} \sum_{i=1}^{N_\Gamma} \tilde{G}_i(j\omega), \tag{4}$$

The response in (4) is employed for obtaining, via standard system identification procedures (Favoreel, De Moor, & Van Overschee, 2000), a minimal state-space realisation of the form

$$\Sigma : \begin{cases} \dot{x}(t) = Ax(t) + B\left(d(t) - u(t)\right), \\ y(t) = v_\theta(t) = Cx(t), \end{cases} \tag{5}$$

with $n \in \mathbb{N}$, $x(t) \in \mathbb{R}^n$ is the state vector, $A \in \mathbb{R}^{n\times n}, \left\{B, C^\mathsf{T}\right\} \subset \mathbb{R}^n$. System (5) constitutes the (approximated) representation of $G(s)$ in (2), obtained from the collected data. The representation in (5), as widely reported in literature (Faedo, Peña-Sanchez, & Ringwood, 2018; García-Violini, Farajvand, Windt, Grazioso, & Ringwood, 2021; Pérez & Fossen, 2008), has to be identified guaranteeing the property of passivity (Zames, 1966), which belongs to the WEC force-to-velocity dynamical behaviour.

4. Estimation of the wave excitation force

This section is dedicated to the description of the adopted strategies for wave excitation force estimation. In particular, the section opens with a brief discussion of the current methodologies employed to estimate the wave signal, and continues with a deeper discussion on the mathematical details of the adopted algorithms.

4.1. Estimation algorithms overview

In literature, many wave estimation techniques have been proposed (Peña-Sanchez et al., 2019). Among these, a first classification comprises receding horizon estimators, observer-based approaches, and data-driven methods (Nguyen & Tona, 2017). The wave motion can be described as a stochastic process, with a distribution which can vary significantly over time (Ochi, 1998), *i.e.* the spectral characteristics of the wave phenomena are different in diverse time lapses during the day. In literature it is proved that model-based state observers constitute an adequate tool for real-time wave excitation force estimation. In this context, the class of observer-based wave excitation force estimators is divided between strategies which do make use of explicit wave models, such as Kalman-Bucy filters (KFs (Kalman & Bucy, 1961)) (Bonfanti et al., 2020; Ling & Batten, 2015), and observers which do not rely on an explicit mathematical model of the wave excitation force, *i.e.* unknown-input observers (UIOs) (Faedo, Bussi, Peña-Sanchez, Windt, & Ringwood, 2021; Nguyen & Tona, 2017). A comprehensive review on state-of-the-art wave excitation force estimators can be found in Peña-Sanchez et al. (2019).

Within this study, the authors adopt and validate the most widespread strategy, *i.e.* the KF approach, and test its effectiveness in an experimental framework, to demonstrate implementability on real systems. In particular, a Kalman-Bucy observer has been tested, based on a random walk (RW), and a harmonic oscillator (HO) wave force model.

4.2. Wave force estimator with Kalman-Bucy filter and random walk model

In this section, the development of a Kalman-Bucy filter for wave excitation force estimation is given. Fig. 2 gives a schematic appraisal of the observer structure. The proposed observer employs an internal model of the wave force, in particular the signal is modelled as a random-walk process, *i.e*

$$\dot{d}(t) = \varepsilon(t), \tag{6}$$

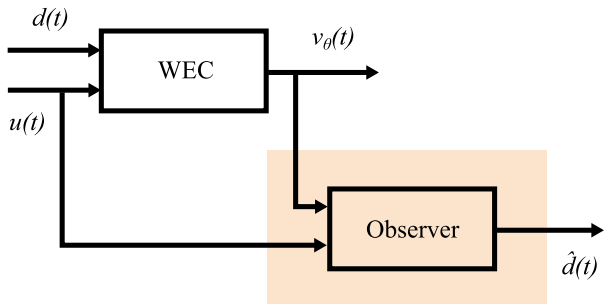

Fig. 2. Wave estimator Kalman-Bucy filter schematic architecture.

with $\varepsilon(t) \in \mathbb{R}$ a white noise component. In a sufficiently general framework, the wave force model can be represented in state space form in terms of the minimal representation

$$\begin{cases} \dot{\xi}(t) = S\xi(t), \\ d(t) = F\xi(t), \end{cases} \tag{7}$$

where $\xi(t) \in \mathbb{R}^\alpha$, and $\alpha \in \mathbb{N}$. (6) is commonly obtained by imposing

$$S = 0, \quad F = \sigma, \tag{8}$$

with $\sigma \in \mathbb{R}$. With reference to (5), it is introduced the augmented system description

$$\begin{cases} \dot{x}_a(t) = A_a x_a(t) + B_a u(t), \\ v_\theta(t) = C_a x_a(t), \\ d(t) = C_d x_a(t), \end{cases} \tag{9}$$

with $x_a(t) = \left[x(t)^\mathsf{T} \xi(t)^\mathsf{T}\right]^\mathsf{T} \in \mathbb{R}^{n+\alpha}$, and

$$A_a = \begin{bmatrix} A & BF \\ 0 & S \end{bmatrix}, B_a = \begin{bmatrix} -B \\ 0 \end{bmatrix}, C_a^\mathsf{T} = \begin{bmatrix} C^\mathsf{T} \\ 0 \end{bmatrix}, C_d^\mathsf{T} = \begin{bmatrix} 0 \\ F \end{bmatrix}, \tag{10}$$

where $A_a \in \mathbb{R}^{n+\alpha\times n+\alpha}, \left\{B_a, C_a^\mathsf{T}, C_d^\mathsf{T}\right\} \subset \mathbb{R}^{n+\alpha}$. The observer structure is given by

$$\begin{cases} \dot{\hat{x}}_a(t) = (A_a - LC_a)\hat{x}_a(t) + Lv_\theta(t) + B_a u(t), \\ \hat{d}(t) = C_d \hat{x}_a(t) \end{cases} \tag{11}$$

with $L = PC_a^\mathsf{T} R^{-1}$, $P \in \mathbb{R}^{n+\alpha\times n+\alpha}$ solution of the algebraic Riccati equation

$$A_a P + PA_a^\mathsf{T} - PC_a^\mathsf{T} R^{-1} C_a P + Q = 0 \tag{12}$$

where $R \in \mathbb{R}, Q \in \mathbb{R}^{n+\alpha\times n+\alpha}$, are the Kalman-Bucy filter tuning parameters.

4.3. Wave force estimator with Kalman-Bucy filter and harmonic oscillator model

An alternative possibility to describe the wave excitation force is to adopt an internal harmonic oscillator model, thus representing the signal as a superposition of different frequency elements generating the wave force. To achieve this, the observer structure remains the same as in Section 4.2, with appropriate changes to the wave force model (7).

Let be $n_\omega \in \mathbb{N}$ the number of frequency components chosen for representing the excitation force, and let the associated set of frequencies be $\mathcal{F} = \left\{\omega_i^{ho}\right\}_{i=1}^{n_\omega}, \omega_i^{ho} \in \mathbb{R}$. With reference to the model in (7), the process and output matrices are defined as

$$S = \bigoplus_{i=1}^{n_\omega} \begin{bmatrix} 0 & \omega_i^{ho} \\ -\omega_i^{ho} & 0 \end{bmatrix}, \quad F = \sigma \mathbf{1}_{2n_\omega}. \tag{13}$$

The remaining observer design steps are the same as those described in (11) and (12).

Table 3
Synthetic spectral characteristics of the wave scenarios.

Sea state	T_p	H_s	γ
SS_1	1.412 [s]	0.063 [m]	3.3
SS_2	1.836 [s]	0.104 [s]	3.3
SS_3	0.988 [s]	0.0208 [m]	1

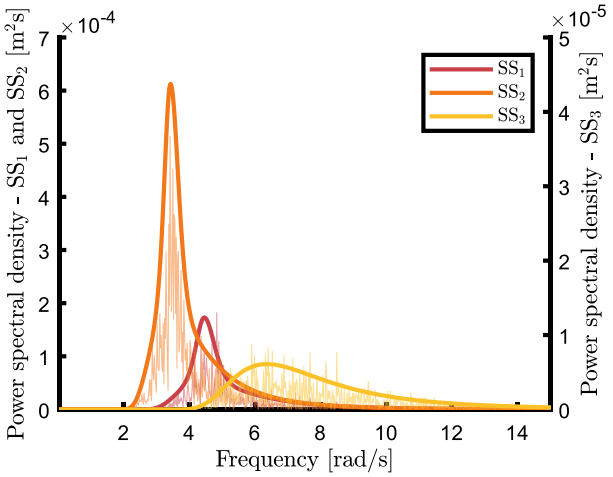

Fig. 3. Sea state spectrum: experimental spectrum (line with transparency) and theoretical spectrum (solid line).

Remark 3. As discussed in Garcia-Abril, Paparella, and Ringwood (2017), the choice of the set $\mathcal{F}$ plays a fundamental role in this wave estimation technique: if the frequency component is not representative enough of the current wave scenario, the excitation estimate will be significantly affected, while if the set includes an excessive number of elements, the system dimension grows rapidly, potentially compromising the real-time hardware implementation of the estimation algorithm.

5. Experimental validation

This section presents the validation tests description and results, both regarding the identification stage in Section 3 and the wave force estimation in Section 4, giving an appraisal of the results obtained in the experimental campaign, and a presentation of the novel proposed observer validation procedure, following with a discussion of the outcomes obtained with the proposed observer strategies.

5.1. Experimental sea states

The experimental tests are performed under irregular wave conditions, *i.e.* the wave elevation signal $\eta(t) \in \mathbb{R}$ is generated on the basis of a JONSWAP spectral stochastic representation (Hasselmann et al., 1973). Three irregular sea states are chosen to validate the estimator algorithm under different representative wave conditions. Each sea state is characterised in terms of significant wave height H_s and typical peak period T_p, a peak enhancement factor γ, and a time length T_{sim}. The wave design parameters for the different sea states are presented in Table 3, while Fig. 3 shows the spectral density function on which the irregular waves are designed, and the actual spectrum obtained from the experiment measurements.

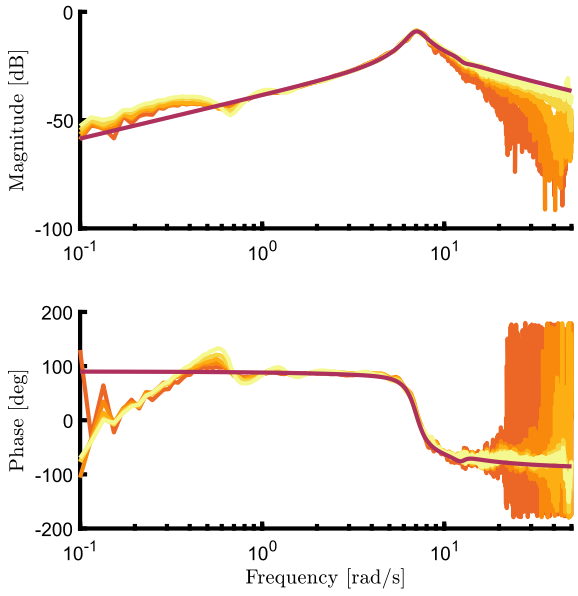

Fig. 4. Bode diagram of the experimental transfer functions. In orange/yellow palette, the ETFE computed for each input tests, and in purple is the average ETFE. (For interpretation of the references to colour in this figure legend, the reader is referred to the web version of this article.)

Table 4
System identification test specification set.

Model order	T_{dc} [s]	N_Γ	Γ [Nm]	Δ [rad/s]
$n = 6$	145	5	[1.5 2.0 2.5 3.0 3.5]	[0.05 15]

5.2. Experimental model validation

Fig. 4 shows the experimental transfer function estimate computed in terms of the system identification procedure presented in Section 3, according to the values in Table 4.

With reference to Fig. 4, yellow and orange lines represent the experimental transfer function relative to each amplitude test in Γ (see Section 3) and the purple continuous line is the average ETFE computed via (4), which can properly characterise the WEC behaviour in the frequency range corresponding with the operating conditions.

For what concerns the validation stage of Eq. (4), as discussed in Section 1, the practical impossibility of measuring the wave excitation force while the system is moving according to the wave motion, presents a practical limit. In fact, the system model validation should be carried out by testing the WEC motion under different irregular sea states, a procedure for which the exact signal acting on the external hull is fully required. For obtaining such input information, following the procedure in Faedo, Peña-Sanchez, Pasta, et al. (2023), the WEC system is 'blocked' in its equilibrium condition by means of the electric motor, which is controlled in position for this task. Within this experimental setup, the excitation force can be measured using the load cell on top of the motor axis. For further details on the system setup in force measurement conditions, the reader can refer to Faedo, Peña-Sanchez, Garcia-Violini et al. (2023), Faedo, Peña-Sanchez, Pasta, et al. (2023).

Fig. 5 shows how the obtained ETFE effectively characterises the uncontrolled (open-loop) motion of the system under the three different irregular sea states listed in Table 3. Additionally, the instantaneous phase error between the model response and the measured angular velocity, under the same input torque condition, which is measured with the 'locking device' procedure, entails a predominant behaviour around the 0° degrees in the considered sea states, implying that the model effectively describes the time evolution of the dynamics under irregular wave forces.

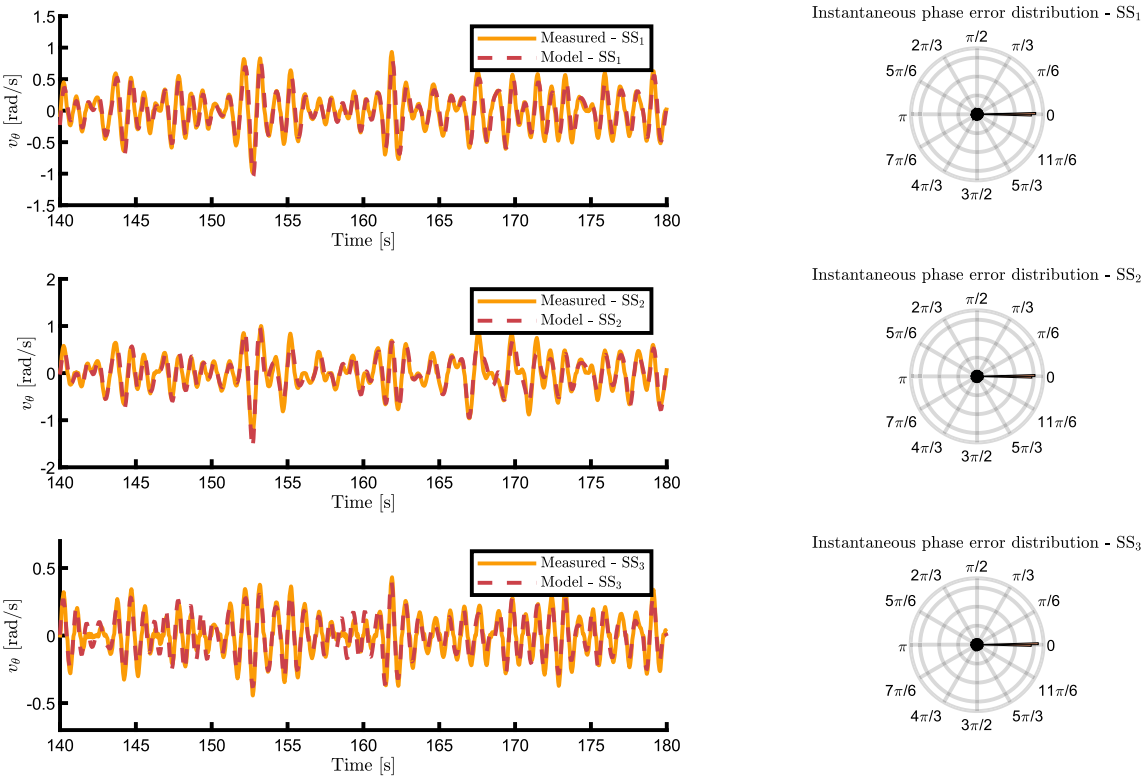

Fig. 5. Validation of the model in (4), with the irregular wave conditions in Table 3. On the left side, an appraisal of the model output (in dashed red) against the measured angular velocity (in yellow), under the same excitation torque conditions, with the discussed 'blocking' strategy. On the right side, the normalised instantaneous phase error distribution of the two signals, expressed in radiant, relative to the sea state on the same figure row. (For interpretation of the references to colour in this figure legend, the reader is referred to the web version of this article.)

5.3. Experimental wave force estimator validation

The first part of this section introduces the framework in which the excitation force observers are tested and validated, while the last paragraphs discuss a numerical appraisal of the obtained results, divided according to the specific evaluation procedure.

In literature, a large part of the experimental validation of wave excitation force estimators exploits the same principle to test the effectiveness of the estimation algorithms (Faedo, Peña-Sanchez, Garcia-Violini et al., 2023; Nguyen & Tona, 2017). Firstly, the wave excitation signal is measured with the 'blocking' procedure while, secondly, the algorithm is tested under the identical wave scenario, comparing the real-time estimate with the expected values. From now on, this strategy is referred to as *open-loop observer validation*. Fig. 6 returns a brief schematic of the discussed procedure with a graphical appraisal of the two stages involved in the process..

Nonetheless, such a validation strategy presents some limits, which hinder the possibility of choosing it as a standard for offshore sea conditions, as discussed in deep in Section 1. In fact, the open-loop method requires that it is possible to reproduce the same excitation force conditions for comparing the estimator output with the actual measured excitation force, assumption which is clearly unreasonable, given that the wave motion cannot be reproduced in the open sea. Furthermore, 'locking' the device itself is often beyond physical realisation.

Driven by this consideration, we propose an alternative procedure for validating the wave excitation force with wider application possibilities, *i.e.*, which can be used in actual sea conditions on real WEC systems. With reference to (2), and considering that the following reasoning can be easily extended to a general WEC force-to-velocity dynamical behaviour, it is clear that, if the control force coincides with the excitation signal, the WEC velocity should be identically 0, *i.e.* the system motion is null. On the basis of this reasoning, the proposed validation procedure consist of injecting the estimated wave excitation signal as the control action, so that, if working correctly, the effective system input is 0, consequently 'cancelling out' the wave excitation force. In other words, if the tested strategy accurately estimates the wave force, the device motion will be 0 for the validation time. Such a method is herein called *closed-loop validation* method. In Fig. 7, the reader can find a brief schematic describing the solution. The novel validation procedure introduces an actual feedback control law in the system, thus the controller stability has to be ensured. In this perspective, it is trivial to prove that system (5) passivity property (see Section 3) ensures the feedback control stability.

Remark 4. The novel validation strategy principle is based on controlling the WEC system with an action which is equal, with an inverse sign, to the estimated wave force, thus limiting to 0 the device motion. Notwithstanding, real estimation algorithms, such as observers, do not estimate exactly the wave excitation signal, but entail an estimation error, which consequently causes a (reduced) motion of the device.

The validation of the strategies described in Section 4, with open-loop and closed-loop criteria, are presented in the following. The tests are performed on the basis of simulations of 300 [s] each.

Open-loop validation. Here is presented the force estimation performance under the three different wave scenarios, by employing in the observer the HO model in (13) and the RW model in (8). The estimator tuning parameters are given in Table 5 and Table 6.

In particular, the frequency set describing the wave excitation force is chosen as the union of the sea states (SS_1, SS_2 and SS_3) typical peak periods (converted in [rad/s] unit).

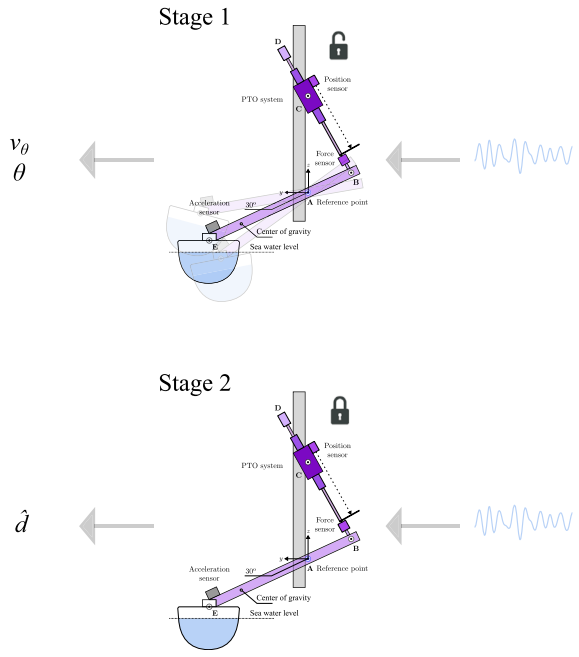

Fig. 6. Experimental setup for wave excitation torque measurement and estimator 'open-loop' validation framework.

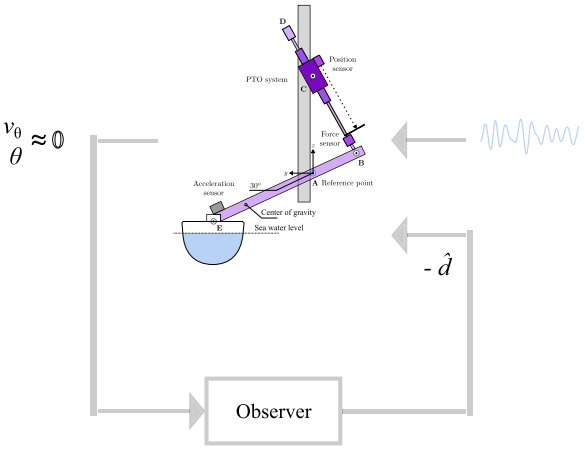

Fig. 7. Experimental setup for wave excitation torque measurement and estimator 'closed-loop' validation framework.

Table 5
Excitation force estimator, harmonic oscillator (HO) version, tuning parameters.

HO observer tuning parameters	
Tuning parameter	Value
R	0.1
Q	$10 \cdot \mathbb{I}_{n+6}$
σ	20
$\mathcal{F}$	2π [1.412 1.836 0.988]$^{-1}$ [rad/s]

Table 6
Excitation force estimator, random walk (RW) version, tuning parameters.

RW observer tuning parameters	
Tuning parameter	Value
R	0.1
Q	$10 \cdot \mathbb{I}_{n+1}$
σ	100

The Figures described in the following give a graphical appraisal of the observer performances, tested with the open-loop validation procedure.

From Fig. 8(a) and 8(b) it can be appreciated how both the HO-based and the RW-based observers are effective in estimating with satisfactory precision the excitation torque at the system hinge, with reference to SS_1, SS_2, and SS_3.

The estimation error slightly worsens in SS_3, given that the identified model is missing some secondary dynamics of the system's actual behaviour under the SS_3 excitation frequency response conditions. Nonetheless, the estimation outcome remains satisfactory, as depicted later in Fig. 9(a) and 9(b).

Despite that the open-loop validation analysis brings promising results for the proposed observers, as discussed in the first part of this section, the applicability of such a validation strategy in open-sea conditions is hindered by the impossibility of replicating a specific excitation force from the primary source and by the practical issues arising in blocking the device in operating scenarios.

Closed-loop validation. In the following *closed-loop* validation strategy, the device motion is driven by a controller which injects in the system the *excitation torque estimate inverse* (*i.e.* with opposite sign), consequently reducing the device motion by counteracting the wave effect. The lower the system motion, the higher the observer's efficiency in estimating the signal. Fig. 9(a) and 9(b) show the results of such validation principle, compared with the actual excitation force signal obtained with the blocking strategy typical of the open-loop approach.

The closed-loop validation strategy brings two significant advantages: the first benefit is the absence of the locking procedure, which can be unpractical, and potentially not possible for every device/concept available. The second aspect regards avoiding the requirement of an exact wave elevation signal repetition, a critical issue which hinders the applicability of the open-loop procedure outside a controlled wave tank environment. In fact, the proposed closed-loop validation is solely based on the instantaneous WEC motion analysis, hence does not require the repetition of any specific wave surface elevation. Additionally, it worth to notice that, since the control force/torque magnitude of a device under optimal control conditions is comparable with that characterising the instantaneous wave excitation force (see *e.g.* Faedo, Peña-Sanchez, Garcia-Violini et al. (2023)), the proposed validation strategy should not experience magnitude limitations, as long as the PTO is effectively designed for such nominal operation conditions.

Remark 5. Note that the PTO systems are equipped with an internal force loop controller, which guarantee tracking of the force requested by the estimators, in the frequency range of interest. The reader is referred to Faedo, Peña-Sanchez, Pasta, et al. (2023) for further details on this internal controller and its tuning.

In Fig. 9(a) and 9(b), the control force is injected into the system in a time window between 80 [s] and 90 [s]. After the control action is introduced, the system motion is heavily reduced and tends to be null (even if, due to the estimation error, a complete motion cancellation is impossible). In this context, the higher the estimation precision, the smaller the oscillation around 0 position. The working principle results are validated with the offline excitation torque measure, which

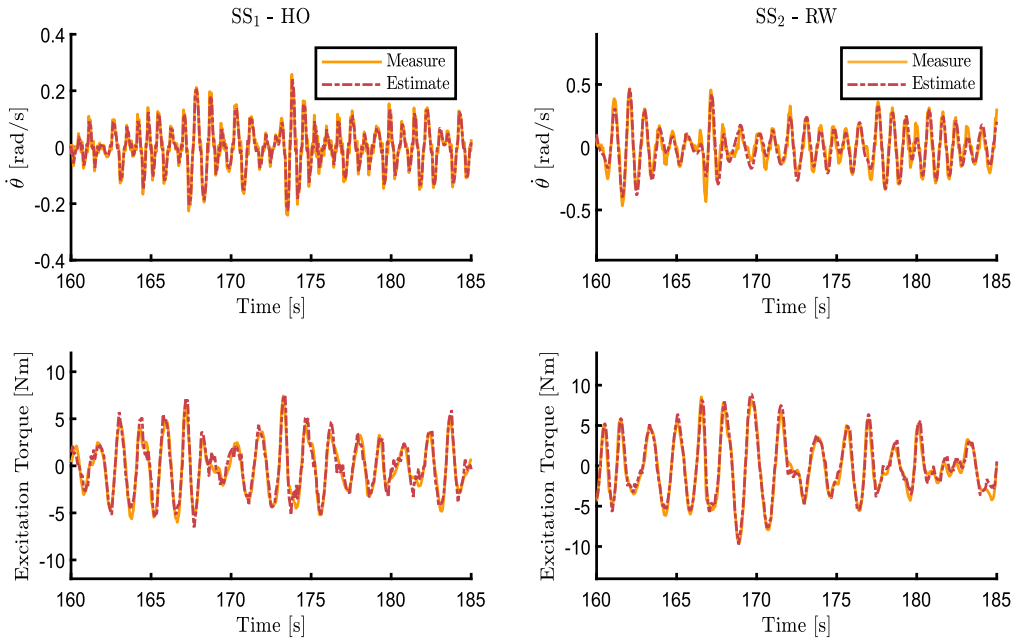

(a) Observer validation: on the upper side, it is shown the velocity estimation output (left the HO observer, tested on SS_1, right the RW observer, tested on SS_2), which allows a reliable recognition of the state estimate quality. On the lower side, the excitation torque estimation performance, referred to the single observer in the specific sea state.

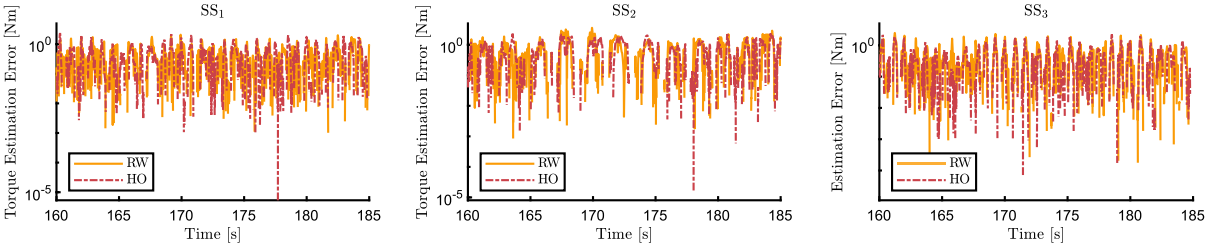

(b) Excitation torque estimation error, in *y*-axis logarithmic scale, of the HO-based and the RW-based observers compared in the three sea state tests described in Table 3.

Fig. 8. Observer validation performance.

is compared with the real-time estimate inserted in the system (with the opposite sign) as control action.

In the estimate results, it can be noticed how, in SS_3 the observer results are slightly less accurate, and hence, the system motion is amplified with respect to the other two tests. This behaviour leads to some consideration both on the closed-loop validation efficiency and the employed model consistency with the system. If the model in (4) accurately describes the WEC dynamics in SS_1 and SS_2, the frequency operational range connected with SS_3 entails a slightly different characterisation of the system, which is partially ignored (or modelled with a poorer precision) by the model. This discrepancy implies a loss in estimation performance, since the observer efficiency relies on the model fidelity. The closed-loop validation strategy can also be employed for checking model fidelity, given that a higher system motion under this closed-loop validation procedure implies a difference between the model (both from the electrical/mechanical and the hydrodynamics side) and the actual physics of the system.

A concise oversight of the open-loop and closed-loop validation strategies is presented in Tables 7 and 8, a step-by-step procedure is offered for validating an excitation force observer, and where advantages and drawbacks associated with each procedure are clearly stated.

6. Conclusions

Driven by the necessity to develop a strategy for assessing and evaluating wave excitation force estimator strategies performance under operative (realistic) conditions, *i.e.* in the open sea with large-scale devices, this study proposes an alternative named closed-loop validation. This latter consists in analysing the device motion under control state, where the action is exactly the inverse of the estimated excitation signal: the reduced such a motion, the higher the estimate quality.

For evaluating the approach effectiveness, two dynamical observers are developed for the WaveStar prototype system, and their estimate quality is tested under classical open-loop procedure, *i.e.* by measuring the excitation force induced by the controlled wave facility tank environment, and under the proposed novel closed-loop validation. For the observer design, the system model is obtained by the use of experimental transfer function estimates, in turn retrieved via properly designed excitation tests. The tests are carried out in real-time, in a controlled tank environment, under three different wave scenarios.

The observers are capable of accurately estimating the wave excitation torque acting on the system hinge, and the closed-loop validation procedure effectively demonstrates the correlation between the estimate quality and the device motion, which is heavily reduced when the observer tracks precisely the wave excitation signal.

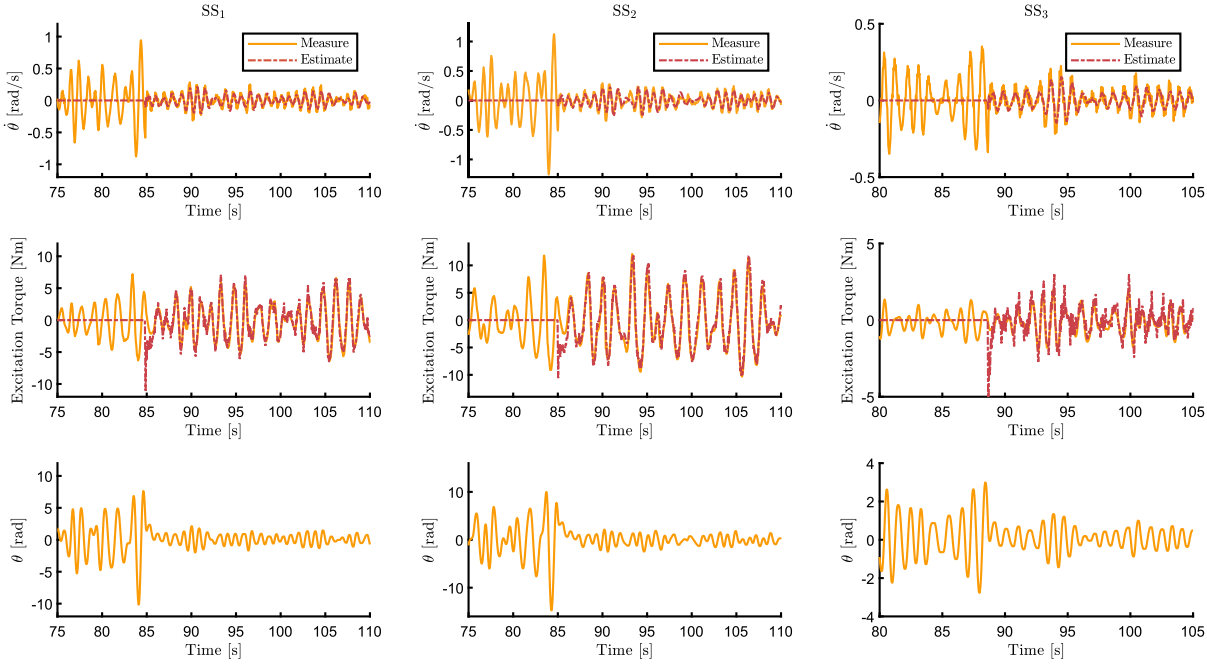

(a) Excitation torque estimation performance, closed-loop validation, RW-based observer. Each column is relative to a specific sea state. The first two rows are the angular velocity and excitation torque estimate, respectively, while the last row is the device position over the test.

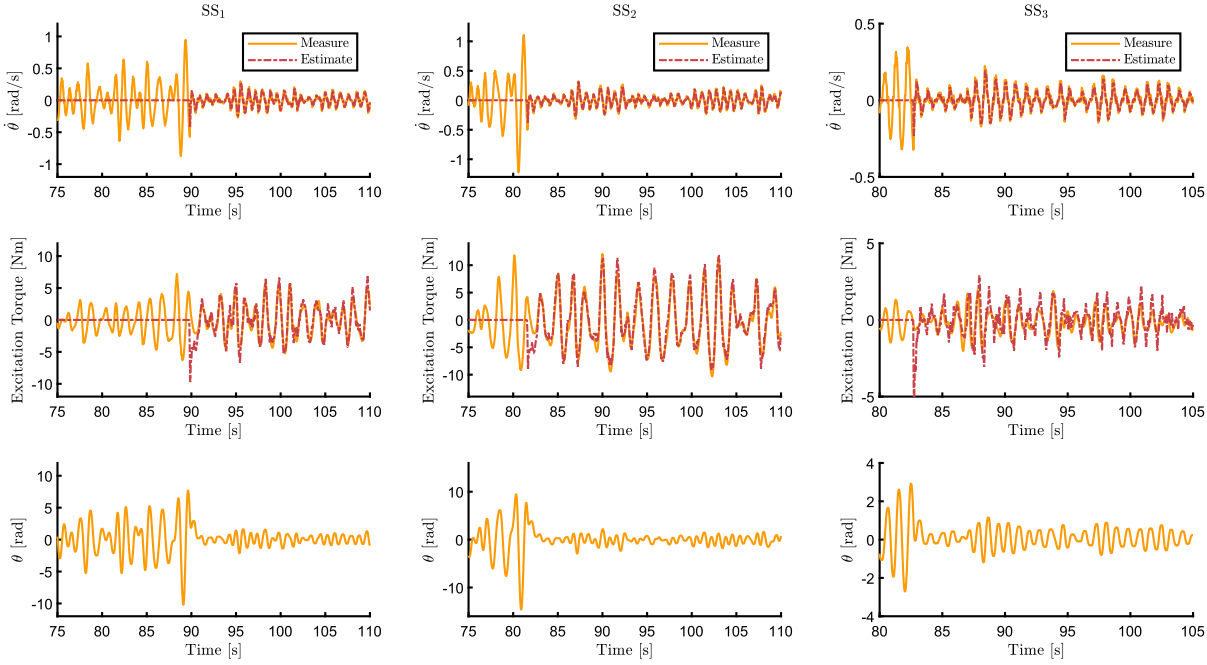

(b) Excitation torque estimation performance, closed-loop validation, HO-based observer. Each column is relative to a specific sea state. The first two rows are the angular velocity and excitation torque estimate, respectively, while the last row is the device position over the test.

Fig. 9. Excitation torque estimation performance.

Table 7
Standard 'blocking' validation procedure of wave excitation force estimators.

Stage 1	
	1. PTO system is disabled. 2. The device is set in free-motion mode. 3. The system is simulated under real wave conditions (*e.g.* SS_1), via the wave maker system. 4. The WEC motion dynamics (position and velocity) are recorded with direct measurements.
Stage 2	
	1. PTO system is disabled. 2. The device is mechanically blocked in hydrostatic equilibrium position. 3. The system is simulated under real wave scenario (*e.g.* SS_1), via the wave maker system. In particular, the experimental setup is required to provide the *exact wave elevation signal* of Stage 1. 4. The excitation force is measured via direct measurement (*e.g.* a load cell placed on the device hinge A, see Fig. 1).
Stage 3	
	1. In simulation environment, the wave excitation force estimator is fed with the motion dynamics obtained in Stage 1, and the force estimate is compared with the force measurement retrieved in Stage 2.
Notes	
	1. It is required the repetition of the exact wave realisation two times, which is not possible in case of real sea scenarios. 2. Blocking the motion of full-scale devices may be not trivial, nor viable.

Table 8
Proposed validation procedure of wave excitation force estimators.

Stage 1	
	1. Enable the PTO system. 2. Provide the PTO *in real time* a control signal which is the *inverse of the excitation force estimate* obtained with the current estimate. 3. Check the device motion, which in perfect estimation scenario should be 0 (in practice, the motion has to stay in a predefined range, since perfect estimation is not trivial to achieve.)
Notes	
	1. Wave repeatability is not required, since the device motion is verified in real-time. 2. System 'blocking' capabilities are not required. 3. Can be employed in real sea condition, on full-scale devices. 4. The observer validation is done in real-time.

CRediT authorship contribution statement

Guglielmo Papini: Conceptualization, Data curation, Formal analysis, Investigation, Methodology, Software, Validation, Writing – original draft, Writing – review & editing, Visualization. **Edoardo Pasta:** Data curation, Funding acquisition, Investigation, Software, Validation, Writing – review & editing. **Yerai Peña-Sanchez:** Investigation, Funding acquisition, Methodology, Data curation. **Facundo D. Mosquera:** Data curation, Investigation, Validation, Visualization. **Demián García-Violini:** Conceptualization. **Francesco Ferri:** Funding acquisition, Investigation, Project administration, Resources, Supervision, Validation, Data curation. **Nicolás Faedo:** Data curation, Funding acquisition, Investigation, Methodology, Project administration, Supervision, Writing – review & editing.

Declaration of competing interest

The authors declare that they have no known competing financial interests or personal relationships that could have appeared to influence the work reported in this paper.

Acknowledgements

Project funded by the European Union - NextGenerationEU under the National Recovery and Resilience Plan (NRRP), Mission 04 Component 2 Investment 3.1 | Project Code: IR0000027 - CUP: B33C22000710006 - iENTRANCE@ENL: Infrastructure for Energy TRAnsition aNd Circular Economy @ EuroNanoLab.

References

Babarit, Aurélien, & Delhommeau, Gérard (2015). Theoretical and numerical aspects of the open source BEM solver NEMOH. In *11th European wave and tidal energy conference*.

Bonfanti, Mauro, Hillis, Andrew, Sirigu, Sergej Antonello, Dafnakis, Panagiotis, Bracco, Giovanni, Mattiazzo, Giuliana, et al. (2020). Real-time wave excitation forces estimation: An application on the ISWEC device. *Journal of Marine Science and Engineering*, *8*(10), 825.

Faedo, Nicolas, Bussi, Ulises, Peña-Sanchez, Yerai, Windt, Christian, & Ringwood, John V. (2021). A simple and effective excitation force estimator for wave energy systems. *IEEE Transactions on Sustainable Energy*, *13*(1), 241–250.

Faedo, Nicolás, Carapellese, Fabio, Papini, Guglielmo, Pasta, Edoardo, Mosquera, Facundo D., Ferri, Francesco, et al. (2023). An anti-windup mechanism for state constrained linear control of wave energy conversion systems: Design, synthesis, and experimental assessment. *IEEE Transactions on Sustainable Energy*, *15*(2), 964 – 973.

Faedo, Nicolás, Giorgi, G., Ringwood, J. V., & Mattiazzo, Giuliana (2022). Optimal control of wave energy systems considering nonlinear Froude–Krylov effects: control-oriented modelling and moment-based control. *Nonlinear Dynamics*, *109*(3), 1777–1804.

Faedo, Nicolás, Peña-Sanchez, Yerai, Garcia-Violini, Demián, Ferri, Francesco, Mattiazzo, Giuliana, & Ringwood, John V. (2023). Experimental assessment and validation of energy-maximising moment-based optimal control for a prototype wave energy converter. *Control Engineering Practice*, *133*, Article 105454.

Faedo, Nicolás, Peña-Sanchez, Yerai, Pasta, Edoardo, Papini, Guglielmo, Mosquera, Facundo D, & Ferri, Francesco (2023). SWELL: An open-access experimental dataset for arrays of wave energy conversion systems. *Renewable Energy*, *212*, 699–716.

Faedo, Nicolás, Peña-Sanchez, Yerai, & Ringwood, John V. (2018). Finite-order hydrodynamic model determination for wave energy applications using moment-matching. *Ocean Engineering*, *163*, 251–263.

Faedo, Nicolás, Peña-Sanchez, Yerai, & Ringwood, John V. (2020). Receding-horizon energy-maximising optimal control of wave energy systems based on moments. *IEEE Transactions on Sustainable Energy*, *12*(1), 378–386.

Falnes, Johannes, & Kurniawan, Adi (2020). *Ocean waves and oscillating systems: Linear interactions including wave-energy extraction*: *vol. 8*, Cambridge University Press.

Favoreel, Wouter, De Moor, Bart, & Van Overschee, Peter (2000). Subspace state space system identification for industrial processes. *Journal of process control*, *10*(2–3), 149–155.

Garcia-Abril, Marina, Paparella, Francesco, & Ringwood, John V. (2017). Excitation force estimation and forecasting for wave energy applications. *IFAC-PapersOnLine*, *50*(1), 14692–14697.

García-Violini, Demián, Farajvand, Mahdiyeh, Windt, Christian, Grazioso, Valerio, & Ringwood, John V. (2021). Passivity considerations in robust spectral-based controllers for wave energy converters. In *2021 XIX workshop on information processing and control* (pp. 1–6). IEEE.

Hasselmann, Klaus, Barnett, Tim P., Bouws, E., Carlson, H., Cartwright, David E., Enke, K., et al. (1973). Measurements of wind-wave growth and swell decay during the Joint North Sea Wave Project (JONSWAP). *Ergaenzungsheft zur Deutschen Hydrographischen Zeitschrift, Reihe A*.

Kalman, Rudolph E., & Bucy, Richard S. (1961). New results in linear filtering and prediction theory. *Journal of Basic Engineering*.

Kramer, Morten, Marquis, Laurent, & Frigaard, Peter (2011). Performance evaluation of the wavestar prototype. In *9th ewtec 2011: proceedings of the 9th European wave and tidal conference, Southampton, UK, 5th-9th September 2011*. University of Southampton.

Li, Guang, Weiss, George, Mueller, Markus, Townley, Stuart, & Belmont, Mike R. (2012). Wave energy converter control by wave prediction and dynamic programming. *Renewable Energy*, *48*, 392–403.

Ling, Bradley A., & Batten, Belinda A. (2015). Real time estimation and prediction of wave excitation forces on a heaving body. In *International conference on offshore mechanics and Arctic engineering*: *vol. 56574*, American Society of Mechanical Engineers, Article V009T09A017.

Mork, Gunnar, Barstow, Stephen, Kabuth, Alina, & Pontes, M. Teresa (2010). Assessing the global wave energy potential. In *International conference on offshore mechanics and Arctic engineering*: *vol. 49118*, (pp. 447–454).

Nguyen, H.-N., & Tona, Paolino (2017). Wave excitation force estimation for wave energy converters of the point-absorber type. *IEEE Transactions on Control Systems Technology*, *26*(6), 2173–2181.

Ochi, Michel K. (1998). *Ocean waves*.

Papini, Guglielmo, Paduano, Bruno, Pasta, Edoardo, Carapellese, Fabio, Faedo, Nicolás, & Mattiazzo, Giuliana (2023). On the influence of mooring systems in optimal predictive control for wave energy converters. *Renewable Energy*, *218*, 119242.

Papini, Guglielmo, Peña-Sanchez, Yerai, Pasta, Edoardo, & Faedo, Nicolás (2023). Optimal control oriented wave surface elevation forecasting strategies: Experimental validation and comparison. In *22nd IFAC world congress 2023: proceeding of the 22nd world congress of the international federation of automatic control, Yokohama, Japan, 9th-14th July 2023*.

Peña-Sanchez, Yerai, Windt, Christian, Davidson, Josh, & Ringwood, John V. (2019). A critical comparison of excitation force estimators for wave-energy devices. *IEEE Transactions on Control Systems Technology*, *28*(6), 2263–2275.

Pérez, Tristan, & Fossen, Thor (2008). Time-vs. frequency-domain identification of parametric radiation force models for marine structures at zero speed. *Modeling, Identification and Control*, *29*(1), 1–19.

Ringwood, John V., Zhan, Siyuan, & Faedo, Nicolás (2023). Empowering wave energy with control technology: Possibilities and pitfalls. *Annual Reviews in Control*.

Scruggs, J. T., Lattanzio, S. M., Taflanidis, A. A., & Cassidy, I. L. (2013). Optimal causal control of a wave energy converter in a random sea. *Applied Ocean Research*, *42*, 1–15.

Twidell, John (2021). *Renewable energy resources*. Routledge.

Zames, George (1966). On the input-output stability of time-varying nonlinear feedback systems part one: Conditions derived using concepts of loop gain, conicity, and positivity. *IEEE Transactions on Automatic Control*, *11*(2), 228–238.